

CAAP Annual Report

Date of Report: *April 7, 2020*

Contract Number: *693JK31850009CAAP*

Prepared for: *U.S. DOT Pipeline and Hazardous Materials Safety Administration*

Project Title: *New Bio-Inspired 3D Printing Functionalized Lattice Composites for Actively Preventing and Mitigating Internal Corrosion*

Prepared by: *North Dakota State University*

Contact Information: *Mr. Xingyu Wang, PhD student, Email: xingyu.wang@ndsu.edu; Mr. Matthew Pearson, M.S. student, Email: matthew.pearson@ndsu.edu, Phone: 701-231-7204; Dr. Hong Pan, Postdoc, Email: hong.pan@ndsu.edu; Mr. Adeeb Ibne Alam, PhD student, Email: adeeb.alam@maine.edu; Dr. Zhibin Lin, Email: zhibin.lin@ndsu.edu, Phone: 717-231-7204; Dr. Bashir Khoda, Email: bashir.khoda @ndsu.edu, Phone: 701-231-7195*

For quarterly period ending: *April 7, 2020*

Business and Activity Section

(a) Generated Commitments

No-cost extension will be made to the existing agreement

Purchase made for the nano-materials, and the 3-D printable polymers

(b) Status Update of Past Quarter Activities

The research activities in the 6th quarter report aimed to complete research activities in Tasks 2 and 3, and continuing efforts on Tasks 5 and 6.

(c) Cost share activity

Cost share was from the graduate students' tuition waiver.

(d) Summary of detailed work for Tasks 2, 3, 5, and 6

Task 2: 3D printing lattice composites

This task aimed to conduct a comprehensive and systematic study of new 3D printing lattice composites through experiment by designing and optimizing 3-D printing structured architecture for desirable mechanical and chemical properties

2.1.1 Step 1: Selection of proper 3D printable materials for 3D printing lattice structures

2.1.1.1 Material pool

In this section, the first attempt was to select proper 3D printable materials. We screened the current polymers as candidates for 3D printable materials, including acrylonitrile butadiene styrene (ABS), polylactic acid (PLA).

2.1.1.2 Sample preparation for bulk samples

Both pre-spoiled polymer filament and raw or granular polymer were purchased from online supplier. Spooled filament came as 2-lb weight and 3-mm diameter, which was fed to the extrusion-based 3D printer used in this research. We made test specimens with a dimension of 2 cm x 2 cm with 10 layers (by a total thickness of 1/2 cm), as shown in **Fig. 1**.

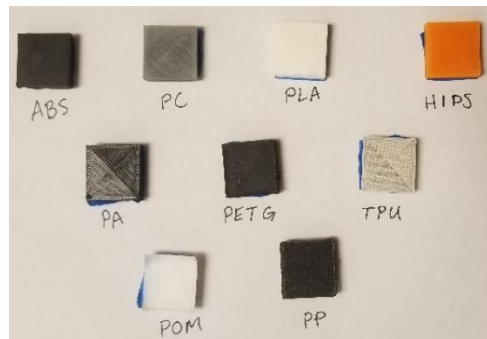


Fig. 1 Samples prepared

2.1.1.4 Contact angle test

3D printing bulk samples were characterized using contact angle test, as illustrated in **Fig. 2**, where the specimen was placed on the test plate and a drop to determine the wettability of the specimens.

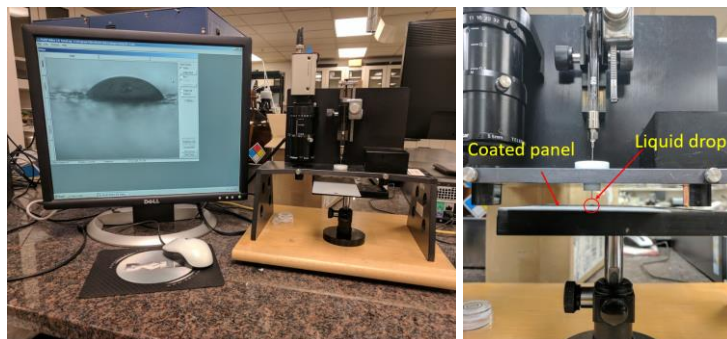


Fig. 2 Equipment used for contact angle test

2.1.2 Step 2: 3-D architecture for 3D printed polymer lattice structures

2.1.2.1 3-D architecture

In this section, we tended to design 3-D architecture to generate 3D printing lattice structures using different patterns. In this project, we attempted to use cubic lattice structure for which the topology will be designed for controlling permeability while maintaining its manufacturability with 3D printing processes, as shown in Fig. 2

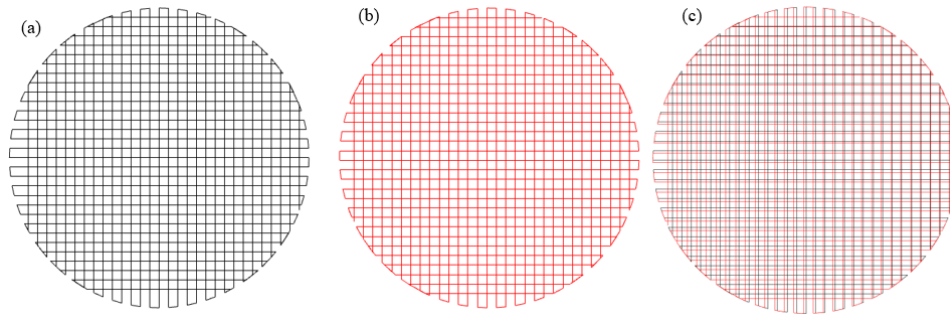


Fig. 2. A single layer 3D filter structure

2.1.2.2 Sample preparation for macro-scale compressive test

This section aimed to understand mechanical behavior of the 3D printing lattice members, including their compressive strength, striving for their damage tolerance against harsh environment that pipeline could experience in real-world applications. Compressive behavior of 3D printing lattice structures could be easily achieved by conducting compression testing of the lattice structure using Instron machine, as illustrated in **Fig. 3**.

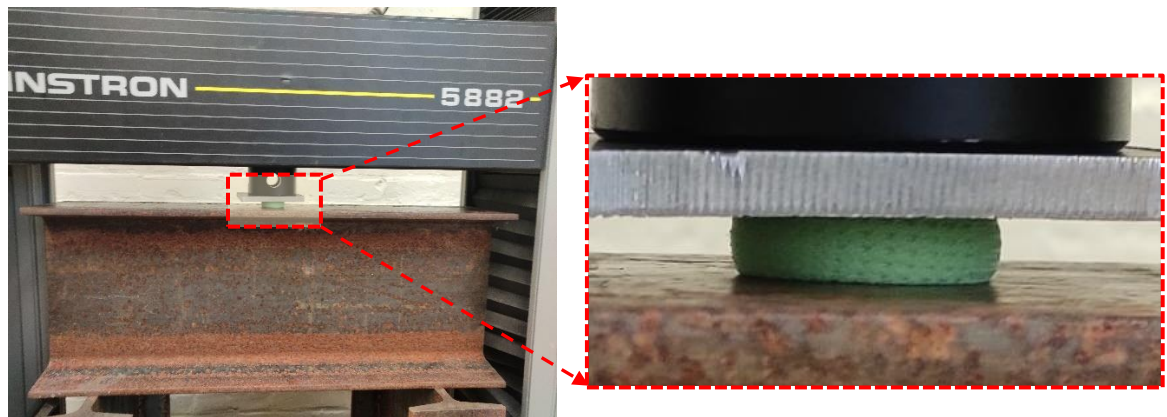


Fig. 3. Compressive testing of the sample

2.1.2.3 Sample preparation for micro-scale nanoindentation test

Besides tensile/compressive strength in macro scale, micro-scale behavior, including indentation, is another key information for mechanical properties of 3D printing samples. To achieve that, atomic force microscopy (AFM) indentation measurement (the Veeco Dimension 3100) was utilized for such characterization, as illustrated in **Fig. 4**. The samples were 3D printing bulk plates with a dimension of 50 mm by 50 mm by 12.7 mm.

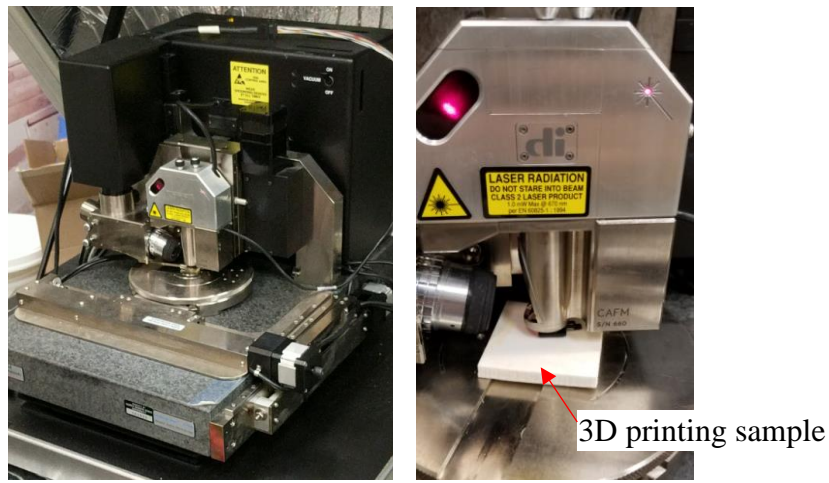


Fig. 4. AFM nanoindentation test of samples

2.1.2.4 Test results and discussion

(a) Macro-scale compressive behavior

The compressive behavior of the 3D printing lattice structures was plotted in **Fig. 5**, where three stages were observed: (a) pre-yielding; (b) plateau; and (c) post strain-hardening behavior.

Before yielded, the latticed behaved nearly linear. As such, Young's modulus of three samples, E_{3D} , were generated with an averaged value of 355 MPa and plotted in **Fig. 6**. Polymeric lattice structures started to yield about 40 MPa. After that, the lattice exhibited a plateau mainly due to compression and close of open cell, and then quickly displayed a strain-hardening behavior due to polymer permanent deformation under high pressure, as commonly observed in polymer compression tests. As illustrated in inserted photos in **Fig. 5**, an initial lattice structure was crushed to a solid disc when approaching the final stage of the loading.

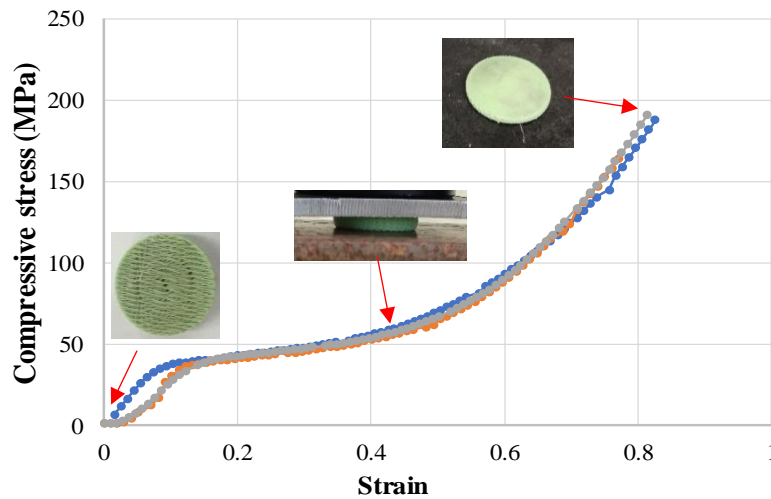


Fig. 5. Compressive stress-strain curve for three samples

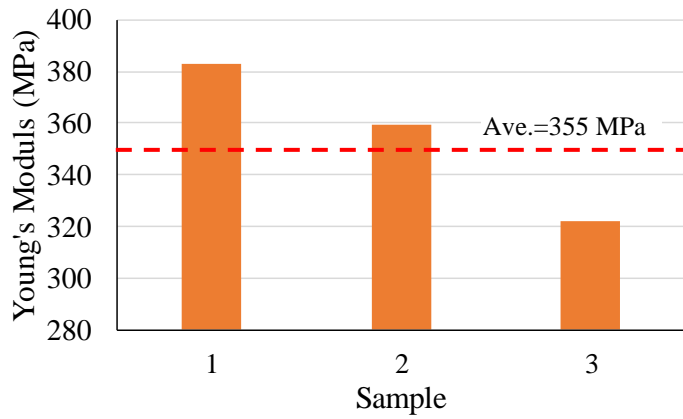


Fig. 6. Young's modulus of the samples (Compression)

(b) Micro-scale indentation behavior

The micro-scale indentation measurement was to understand the resistance of the 3D printing structure to a deformation when an applied loading performed indentation tests through the indenter in force mode. Thus, the level of indentation modulus (elastic modulus) of the 3D printing samples responded for the capacity of restoration of unloading. As shown in **Fig. 7**, test samples were in well consistent with an averaged value of 1568 MPa.

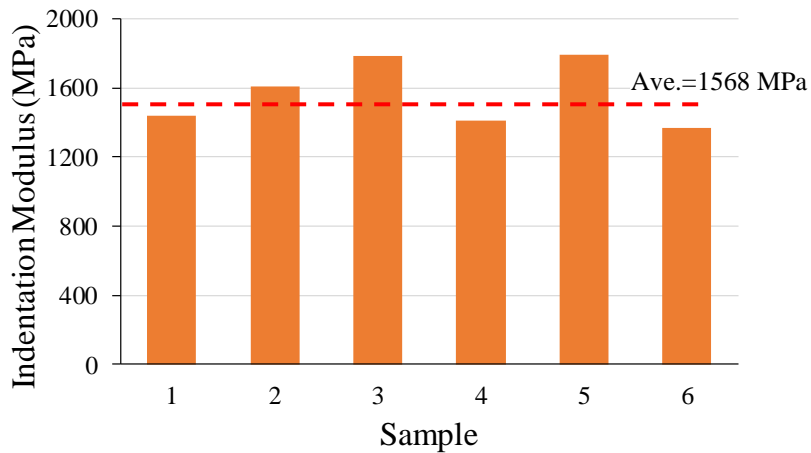


Fig. 7. Elastic modulus of the samples (Indentation)

2.2.1 Step 3: Optimization of 3-D architecture for 3D printed polymer lattice structures

The lattice structures were printed, while the porosity generated created open cell lattice type architecture. In the first trial, 1.75 mm PLA filament is printed with 0.4-inch (0.4 mm) nozzle size in a open source Creality printer (Creality Ender-3 Pro). The temperature at the bed is used at 70 deg, and nozzle temperature is set at 205 deg F (deg Celsius) during the print. The sample print has a height of 0.56-inch and 40 layers and the diameter as 1 inch. We used an upgraded glass bed instead of a removable magnetic bed. The filament diameter used in this printer is 1.75mm and the filament was from amazon basics. To control the porosity and the pore size, besides R-type and LS-type patterns used in the Section 2.1.2, we also proposed all-in-one patterns for optimization.

Clearly, the concept of the lattice structures used in section (a) or (b) was based on either R-type or LS-type with stacked multiple layers to form a composite system. Such fixed pore sizes could limit their applications to certain situations. For instance, pores at the exterior layers should be relatively larger so as to reduce the flow pressure during their filtering, while pore sizes interior require relatively smaller.

We proposed all-in-one hierarchic lattice structures to accommodate different fluid particles flowing through different sizes of pores, and gradually separate them along different sizes, with a pre-defined

raster width, where each layer with different pore sizes was rotated along the build axis as shown in **Fig. 8** and stacked in sequence to build the 3D structure.

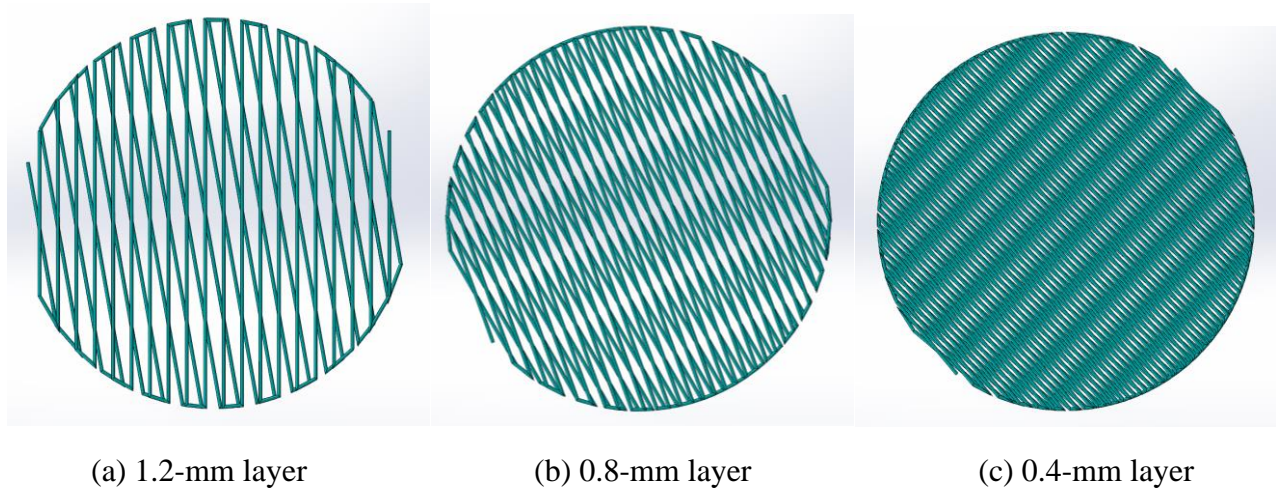


Fig. 8 Layers with different pore sizes.

Task 3: Materials to functionalize the 3-D printing composites

This task aimed to conduct a comprehensive study to screen, characterize, and optimize surface treatment materials that are capable of serving as functional groups using different chemical compositions for new 3D printing lattice structures.

3.2.1 Step 1: Characterization of selected surface treatment materials in terms of bond behavior

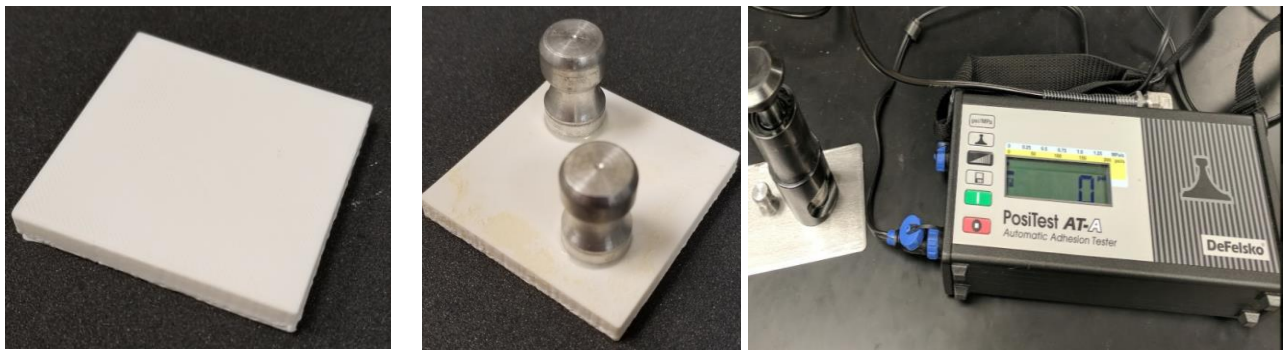
3.2.2.1 3D printing bulk sample preparation and test setup

Consider that it is hard to conduct the adhesion test of surface treated 3D printing lattices, where pore size distribution could affect the measurement. Instead, this step attempted to catch the information of bond behavior of surface treatment materials with 3D printing bulk substrate. As shown in **Fig. 9(a)**, the samples were 3D printing bulk plates with a dimension of 50 mm by 50 mm by 12.7 mm.

The adhesion test of samples, illustrated in **Fig. 9(b)**, were loaded on standardized machine, PosiTest AT-A, in accordance with ASTM C1583/D4541. Dollies were glued to the test specimens, and the pull-off strength was measured during the experiment. The test was performed 24 hours after the dollies were applied. Adhesion tester was used to apply tension load normal to the test surface, while the pull-off strength (adhesion) was measured and recorded when the dolly was detached from the surface.

3.2.2.2 Bond behavior of surface treatment materials to 3D printing substrate

The pull-off strength (adhesion) to 3D printing substrate was measured by following ASTM D4541. The test results were plotted in **Fig. 10** where the averaged adhesion strength of the surface treatment materials to the 3D printing substrate was 1.58 MPa. Clear observation after measurement, illustrated in **Fig. 10(a)**, revealed that de-bonded surface was from 3D printing sample, suggesting that the bond between surface treatment materials and 3D printing substrate is sufficient. **Fig. 10(b)** also confirmed a rougher surface profile captured by AFM classification after bond test was associated with delamination of 3D printing layers.



(a) Test PLA sample

(b) Setup for adhesion test

Fig. 9. Adhesion test for bond behavior of surface treatment materials with 3D printing substrate

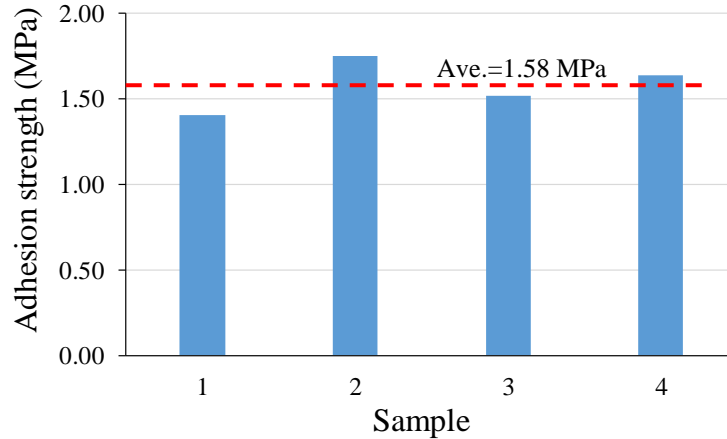


Fig. 10. Adhesion strength of samples

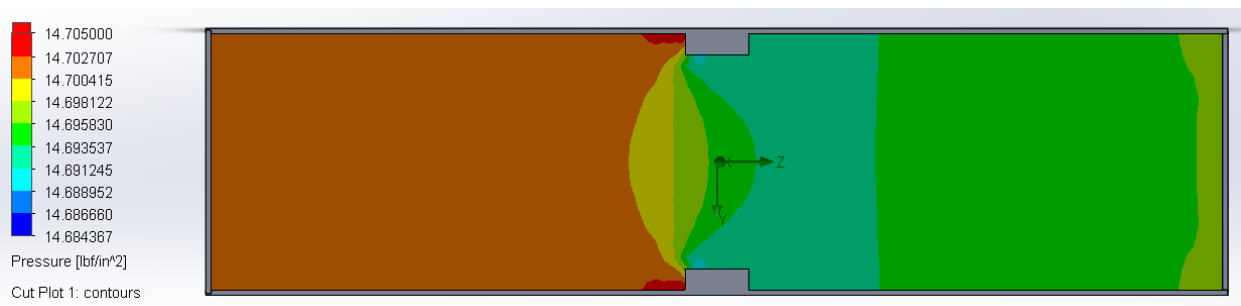
Task 5: Characterize the new composite systems

This task aimed to conduct a comprehensive experimental investigation to characterize the properties of the new 3D printing lattice composite system and particularly the features of characterize and optimize the chemical activities of the new 3-D printing composites

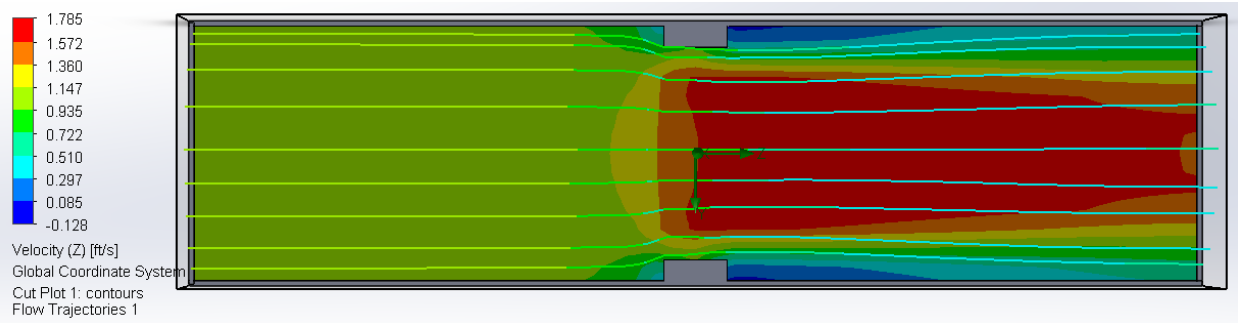
- Numerical simulation to identify and optimize the design parameters

Finite element method (FEM), as a numerical tool, was used to simulate a similar situation with the real state. The three-dimensional (3-D) pipes under different cases were modeled, where mixed water and hexadecane were considered.

As typically illustrated in **Figs. 11a and 11b**, the results of the Finite Element Method were presented and discussed in Section 3.



(a) Pressure contour



(b) Velocity contour

Fig. 11 FE results of the pipe under different cases.

5.1 Continuous efforts on design of 3D printing lattice structures

We developed a customized multi-material delivery system to print the porous structure with lattice architecture within five-micron spatial accuracy. As well known, periodic cellular structure is the most known man-made cellular structure which are used in the design of light weight sandwich panel structures.

5.2 Continuous efforts on composites

We selected the PLA and ABS as our base for printing materials in that there were no preferable 3D printable materials so far.

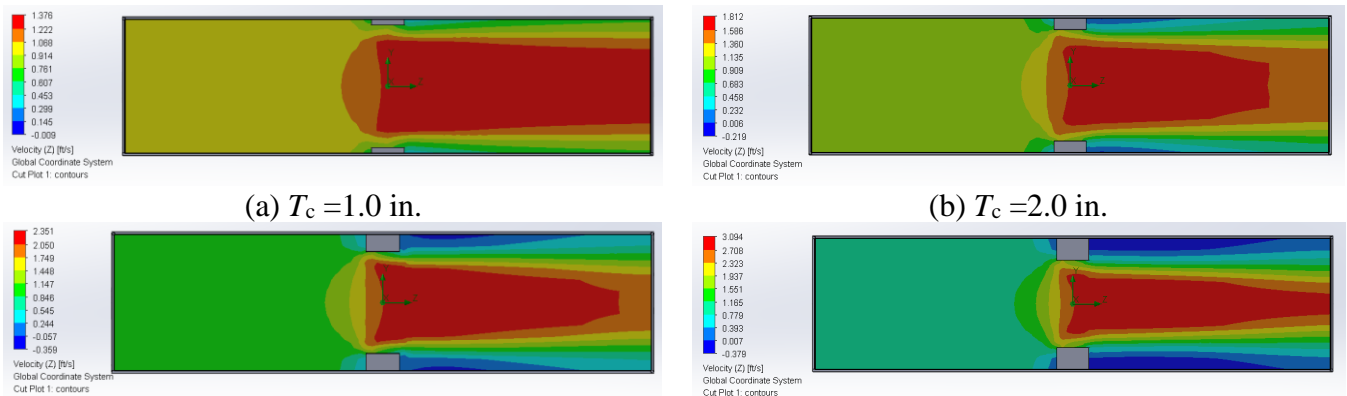
Surface morphologies of pristine samples and modified ones were observed by Scanning Electron Microscopy (SEM, JEOL, Japan) and the elemental distribution of the as-prepared samples were investigated by Energy-dispersive X-ray Spectroscopy (EDS) attached to SEM.

5.3 Results and discussion

5.3.1 Effects of the composite thickness on the flow conditions

This group of the simulation was to understand the impacts of composite thickness on the flow conditions, and the findings could help to design the composite layers.

Figs. 12 and 13 were plotted in the cross-sectional view in contour, where flow velocity was 1.0 ft/s and initial pressure was about 15 psi, and pipe dimension was 24-in in diameter. Clearly, the flow conditions (velocity or rate in **Fig. 12** and pressure in **Fig. 13**) were disturbed near the location of the composite layers. With the increase of the thickness, the initial flow rate raised up to over 3 times higher at the narrow pathway than those at other locations, particularly when at the composite layer of $T_c = 4.0$ in as expected. Differently, the flow pressure was less disturbed by the composite layers by less 0.2% over all cases, with slightly more uniformly distribution over the whole flow. Note that the fluid viscosity (friction) such as oil type fluid was not considered in this stage, and we will discuss that in the further study.



(c) $T_c = 3.0$ in.

(d) $T_c = 4.0$ in.

Fig. 12 Impacts of different composite thickness on the flow conditions (velocity) by $D_p=24$ -in dia.

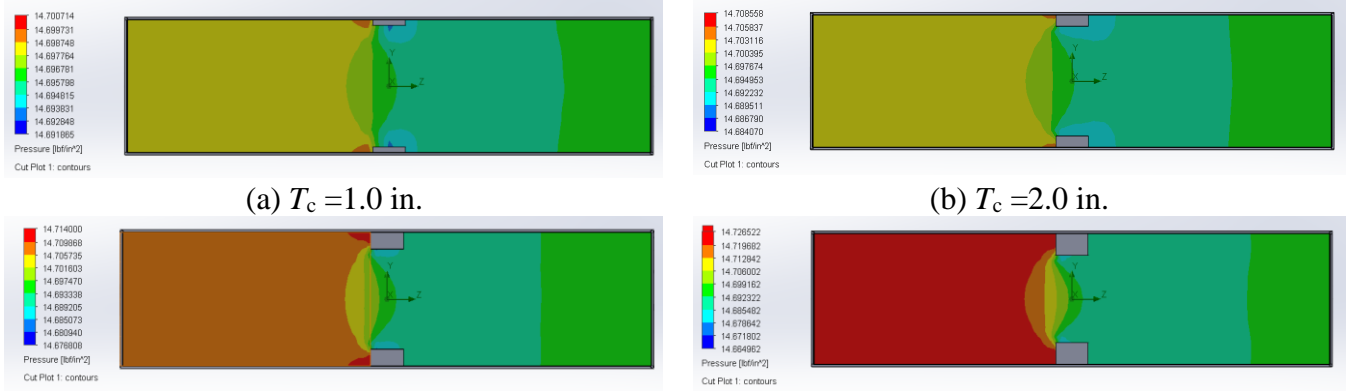
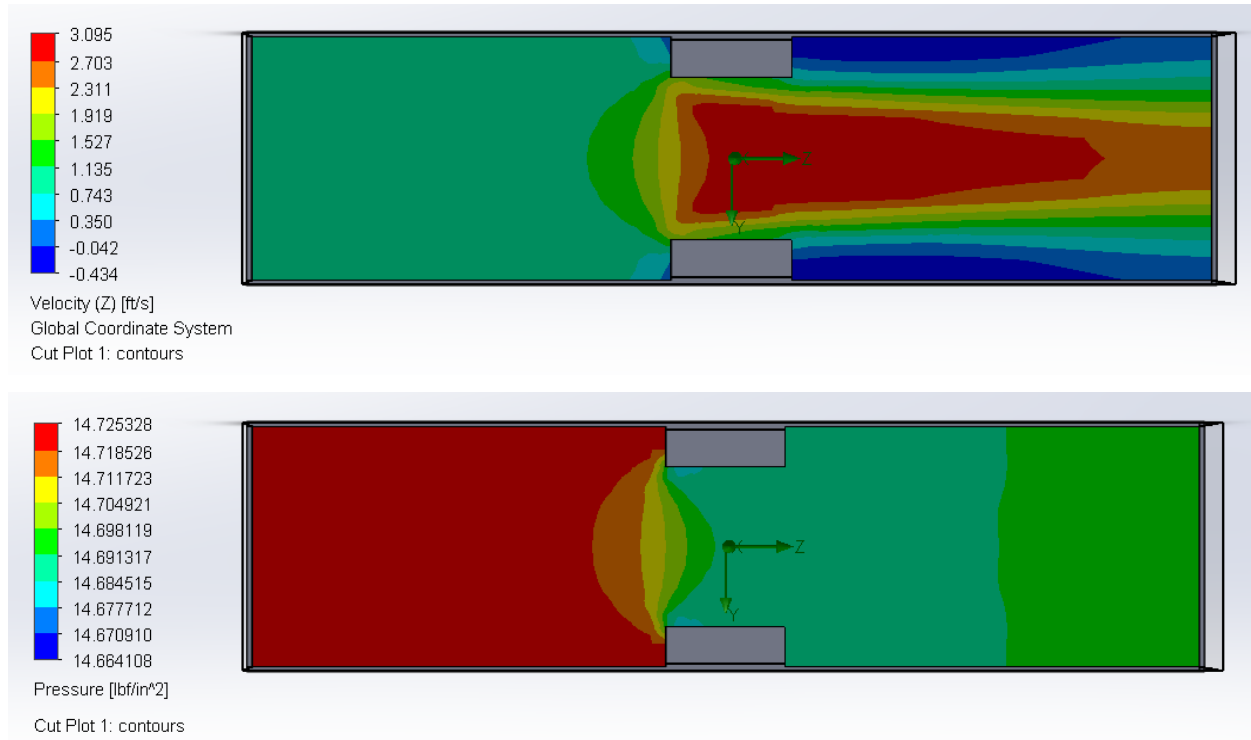


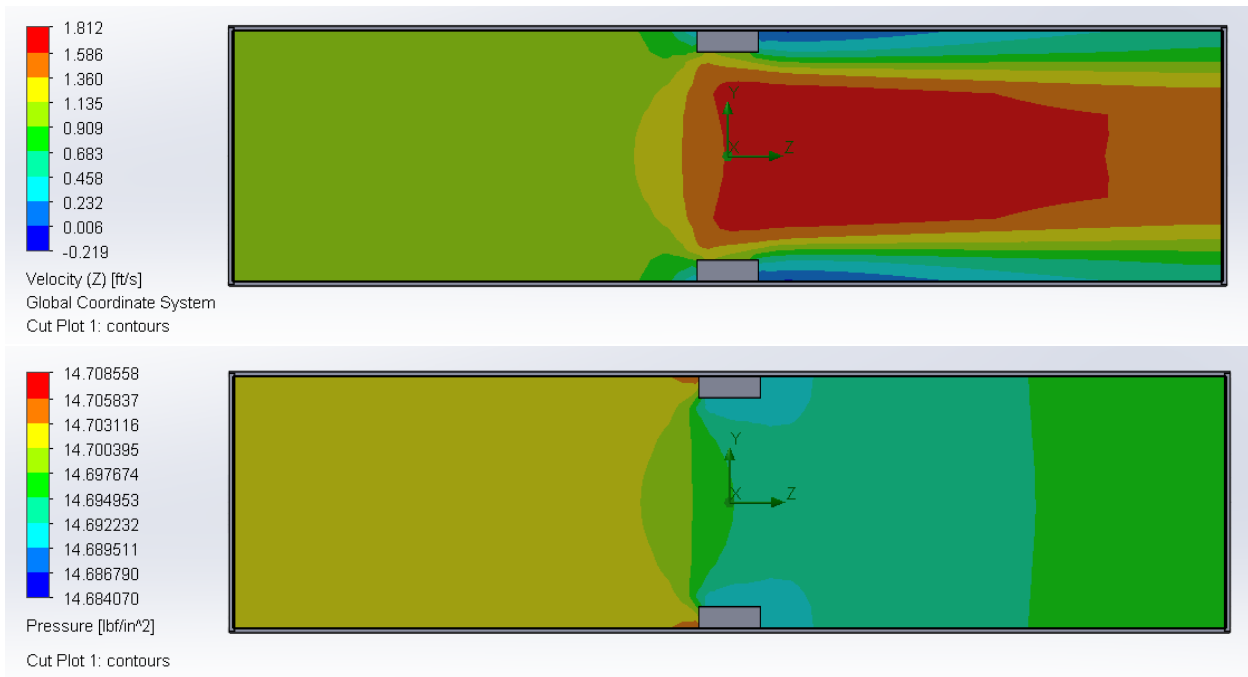
Fig. 13 Impacts of different composite thickness on the flow conditions (pressure) by $D_p=24$ -in dia.

5.3.2 Effects of the diameter size on the composite layers

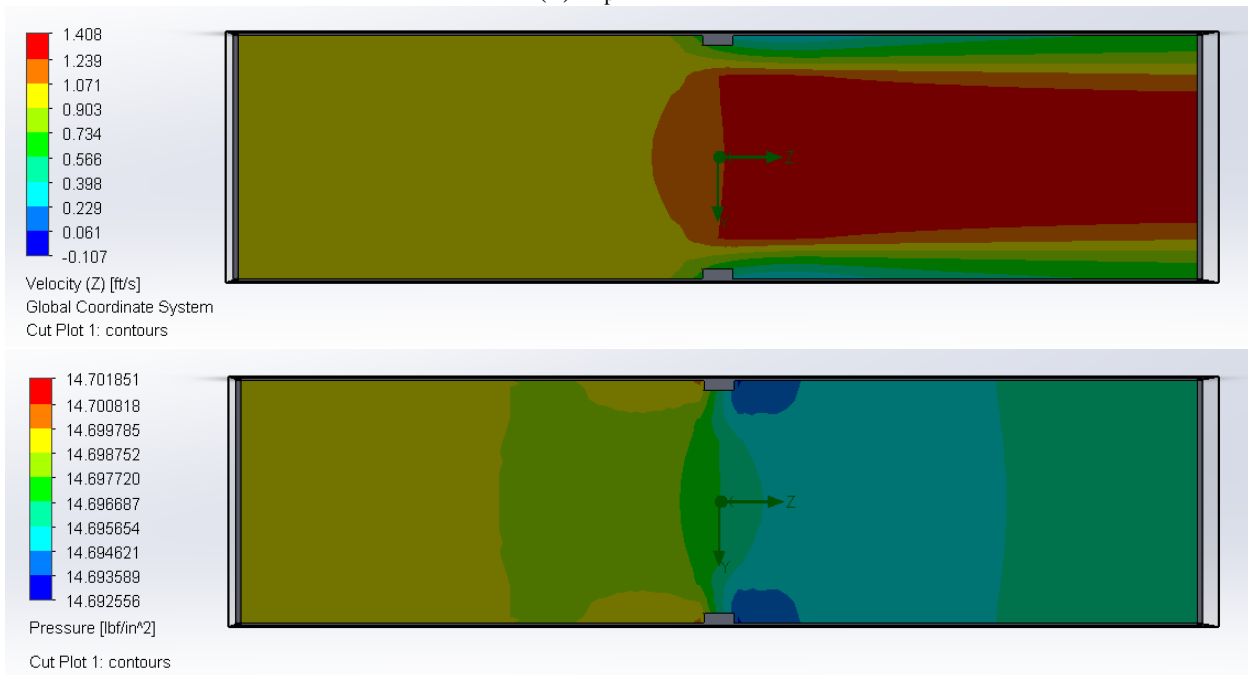
To better qualitatively determine the effectiveness of the composite layers under varying pipe sizes, three typical sizes, 12-, 24-, and 48-in diameters, were selected from small to large scale pipes. The results were shown in **Figs.14 and 15**, where different diameters and different composite thickness were presented. Clearly, with the increase of the pipe size, the composite layers have less sensitivity to flow conditions (velocity and pressure).



(a) $D_p = 12$ in.

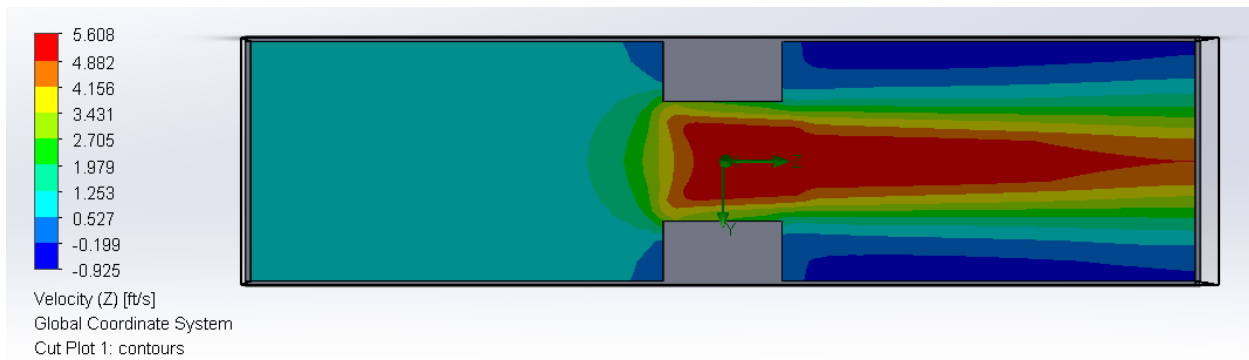


(b) $D_p = 24$ in.

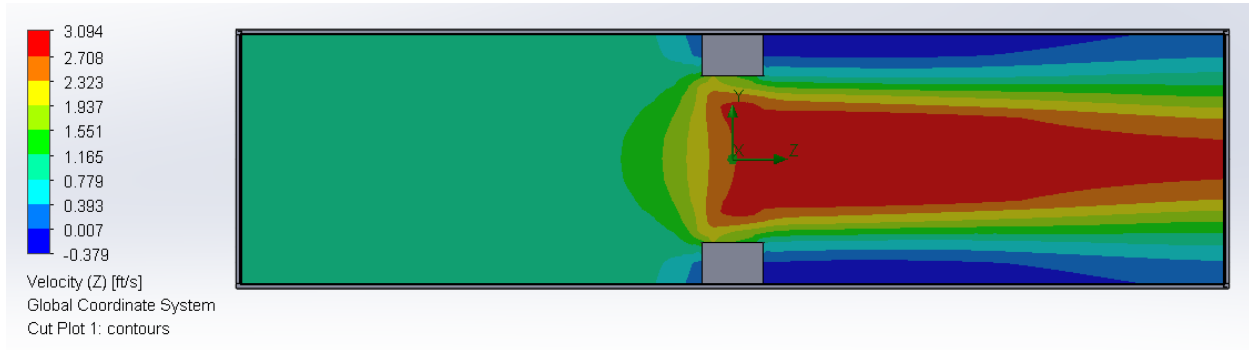


(c) $D_p = 48$ in.

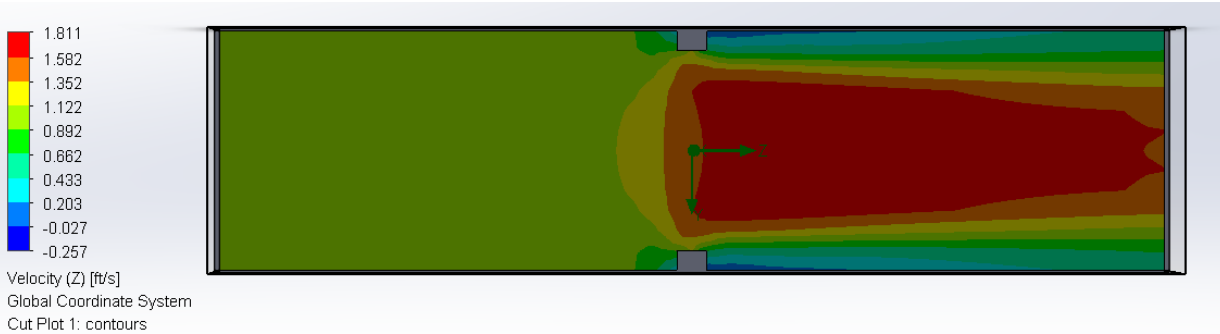
Fig. 14 Impacts of pipe sizes on the composites by $T_c = 2.0$ in.



(a) $D_p = 12$ in.



(b) $D_p = 24$ in.



(c) $D_p = 48$ in.

Fig. 15 Impacts of pipe sizes on the composites by $T_c = 4.0$ in.

5.3.3 Effects of the initial flow velocity on the performance of the composite layers

Consider that actual gas pipe could use the initial velocity reach up to 30~60 ft/s, the initial flow velocity could affect the performance of the composite layers on the internal surface of a pipe. The results were shown in **Fig. 16**. The major trend in the flow conditions (velocity and pressure) was identical. The resulting flow velocity was approximately proportional to the amplitude of the initial flow rate, while the resulting flow pressure, illustrated in **Fig. 17**, raised with the increase of the flow velocity as expected.

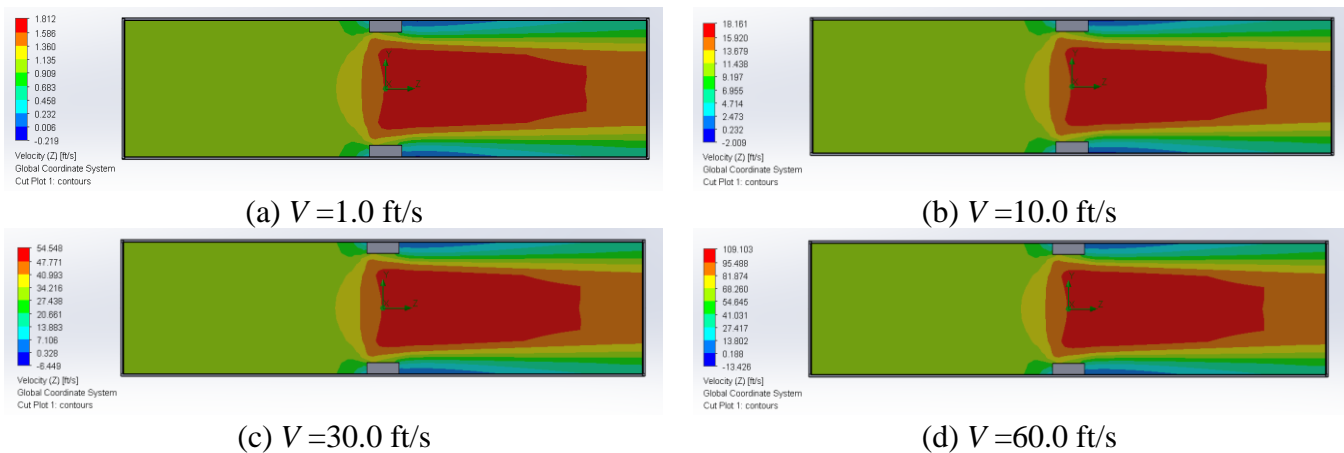


Fig. 16 Impacts of flow velocity on the composite layers by $D_p = 24$ -in dia.

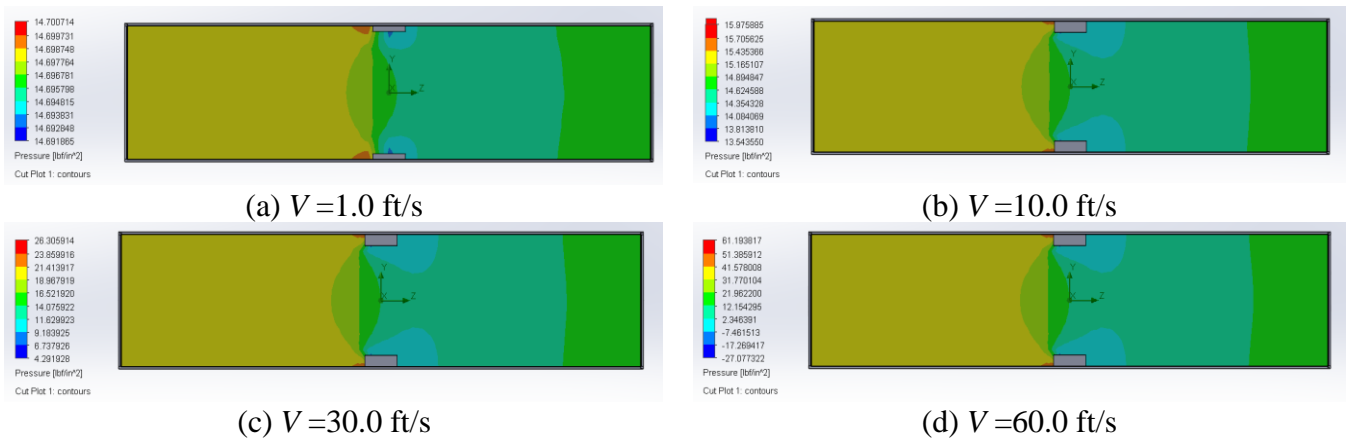


Fig. 17 Impacts of flow velocity on the composite layers by $D_p=24$ -in dia.

Task 6: Durability tests of the new composite systems

This task aimed to understand the durability and associated physical and chemical change of the 3D printing lattice composites under the accelerated conditions.

6.1.1 Degradation in terms of mass loss due to abrasion

Consider that the 3D printing composite systems could expose to wear/abrasion during the operation, we attempted to understand the degradation in terms of mass loss due to fluid abrasion. To qualitatively reflect such degradation, we attempted to use standardized abrasion test, in accordance with ASTM D4060 (the constant load of 1000 g used during the test and the rotational speed of 72 rpm with two CS-10 abrading wheels).

6.1.2 Degradation in terms of mass loss due to abrasion

The test samples exhibited relatively high abrasion resistance at initial 100 and 200 cycles. The mass loss reached up to 2.8 times when loaded cycles approached 500, and reached a slightly plateau at 1000 cycles. The samples exhibited relatively high mass loss at 2000 cycles.

(e) Description of any Problems/Challenges

No problems are experienced during this report period

(f) Planned Activities for the Next Quarter

The planned activities for next quarter are listed below:

- More efforts on investigation of degradation associated with pressure, including design and characterization of pump-induced pressure and its impacts on the designed composite systems.
- Continuing efforts on characterization of durability of all-in-one heterogenous stacked layers;